Supporting Information

Hirota et al. 10.1073/pnas.1009324107

SI Materials and Methods

2D-DIGE Analysis and Protein Identification. DeCyder v6.5 software (Amersham Biosciences) was used for simultaneous comparison of abundance changes across all 10 samples with statistical confidence. Data reduction by principle components analysis demonstrated that in *ca*. 100 intact protein features that changed significantly ($P < 0.01$, ANOVA) among these three genotypes across all samples, the major source of variation (PC1 = 63.5) separated the PR-null ($Pgr^{-/-}$) samples from the others, and the second greatest source of variation (PC2 = 24.4) separated the remainder of the samples by WT vs. FK506-binding protein 52-deficient ($Fkbp52^{-/-}$). These results provided additional confidence that the observed changes were reflective of the biology rather than arising from unanticipated experimental or biological variation. Proteins of interest were robotically excised and processed for MS analyses using an Ettan Spot Handling Workstation (GE Healthcare). MALDI-TOF MS and TOF/TOF tandem MS were performed on a Voyager 4700 (Applied Biosystems) using data-dependent tandem MS acquisition on the 20 most abundant ions in each MALDI-TOF peptide mass map. MALDI-TOF peptide mass maps and accompanying tandem mass spectra then were collectively searched against the Swiss-Prot and NCBInr databases using GPS Explorer software (Applied Biosystems) running the Mascot database search engine (Matrix-Science). Searches were performed without constraining protein molecular weight or isoelectric point and allowed for carbamidomethylation of cysteine, partial oxidation of methionine residues, and one missed trypsin cleavage. Identifications were accepted based on a tripartite evaluation that takes into account significant molecular weight search (MOWSE) scores, spectrum annotation, and observed vs. expected migration on the 2D gel (1).

1. Friedman DB, et al. (2004) Proteome analysis of human colon cancer by two-dimensional difference gel electrophoresis and mass spectrometry. *Proteomics* 4: 793–811.

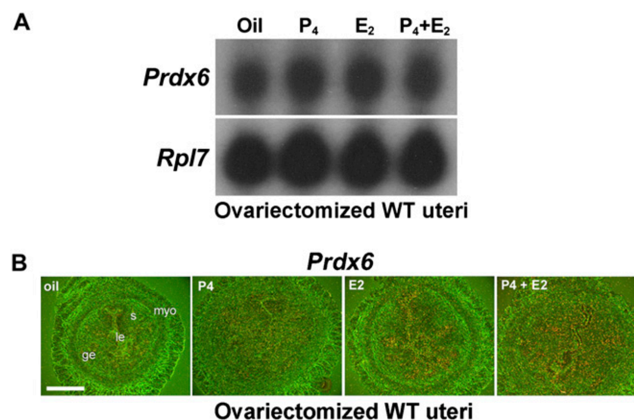

Fig. S1. Effects of progesterone (P_4) and/or estradiol-17β (E_2) on peroxiredoxin-6 (*Prdx6*) expression in ovariectomized WT uteri. (*A*) Expression levels of uterine *Prdx6* mRNA in ovariectomized CD1 WT mice treated with oil (vehicle), P_4, E_2, or P_4+E_2 for 24 h as determined by Northern hybridization. *Rpl7* was used as a loading control. (*B*) In situ hybridization showing differential patterns of *Prdx6* expression in ovariectomized CD1 WT uteri treated with oil, P_4, E_2, or P_4+E_2. ge, glandular epithelium; le, luminal epithelium; myo, myometrium; s, stroma. (Scale bar, 200 μm.)

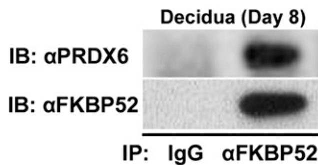

Fig. S2. Physical association of FK506-binding protein 52 (FKBP52) with PRDX6 in day 8 decidua. Decidual cell protein extracts were immunoprecipitated with an anti-FKBP52 antibody. Pulled-down complexes were run on SDS/PAGE and immunoblotted using antibodies specific to PRDX6 or FKBP52. The control immunoprecipitation (IP) was performed by incubating protein lysates with a rabbit IgG. IB, immunoblotting.

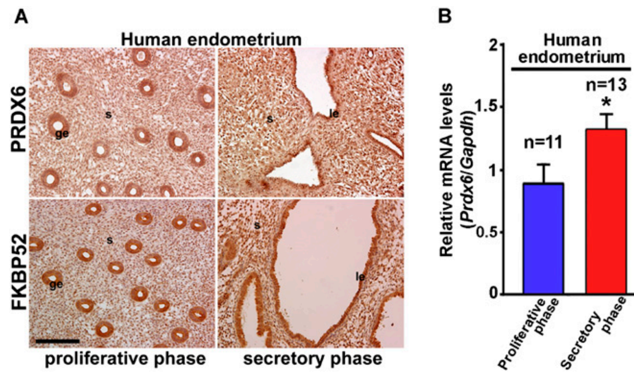

Fig. S3. PRDX6 expression in the human endometrium. (*A*) Immunostaining of PRDX6 and FKBP52 in human endometrium. Brown deposits indicate sites of positive immunostaining. ge, glandular epithelium; le, luminal epithelium; s, stroma. (Scale bar, 200 μm.) (*B*) Expression levels of *Prdx6* mRNA are higher in the secretory phase of human endometrium than in the proliferative phase. The number of samples assessed is indicated above each bar. Values are mean ± SEM. **P* < 0.05.

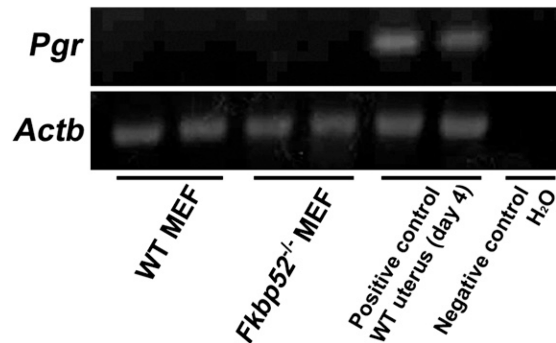

Fig. S4. Progesterone receptor (*Pgr)* mRNA is undetectable in mouse embryonic fibroblasts (MEFs). Undetectable levels of *Pgr* mRNA in WT and *Fkbp52*$^{-/-}$ MEFs as determined by RT-PCR. *Actb* served as an internal control. WT uteri at day 4 of pregnancy and water were used as positive and negative controls, respectively.

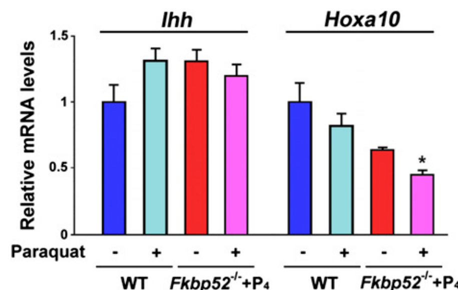

Fig. S5. Paraquat reduces *Hoxa10* expression in *Fkbp52*$^{-/-}$ uteri on day 4 of pregnancy. Expression levels of *Ihh* and *Hoxa10* mRNA in paraquat-treated uteri from WT and P_4-primed *Fkbp52*$^{-/-}$ mice on day 4 of pregnancy as determined by Northern hybridization are shown. Band intensities of *Ihh* and *Hoxa10* were normalized against *Rpl7*. *Fkbp52*$^{-/-}$ females were treated with P_4 (2 mg/d) on days 2–4 of pregnancy. Paraquat was injected on the evening (1800 hours) of day 3 of pregnancy. Two or three independent samples from different mice were examined in each group. Data are given as mean ± SEM. **P* < 0.05 compared with P_4-primed *Fkbp52*$^{-/-}$ mice without paraquat.

Table S1. Proteins down-regulated selectively in *Fkbp52*$^{-/-}$ uteri

Protein identification	Accession number	MW pl	WT vs. *Pgr*$^{-/-}$ Av ratio	WT vs. *Pgr*$^{-/-}$ *P* (*t* test)	WT vs. *Fkbp52*$^{-/-}$ Av ratio	WT vs. *Fkbp52*$^{-/-}$ *P* (*t* test)	*Pgr*$^{-/-}$ vs. *Fkbp52*$^{-/-}$ Av ratio	*Pgr*$^{-/-}$ vs. *Fkbp52*$^{-/-}$ *P* (*t* test)	*P* (ANOVA)
FK506-binding protein 52 (FKBP52)	P30416	51.8 5.5	1.04	0.75	−3.62	0.0005	−3.77	0.0004	0.00006
Peroxiredoxin-6 (PRDX6)	O008709	24.8 5.7	1.01	0.77	−2.01	0.04	−2.02	0.00004	0.036

Accession numbers in Swiss-Prot database were used. Theoretical molecular weight (MW, in kDa) and isoelectric point (pl) are calculated from the database entries, which often contain precursor sequences not present in the mature form migrating on the gel. Average volume ratios (Av ratio) and *P* values of Student's *t* test and ANOVA were calculated using DeCyder software version 6.5, using mixed-sample internal standard methodology.

Table S2. Proteins up-regulated selectively in *Fkbp52*$^{-/-}$ uteri

Protein identification	Accession number	MW pl	WT vs. *Pgr*$^{-/-}$ Av ratio	WT vs. *Pgr*$^{-/-}$ *P* (*t* test)	WT vs. *Fkbp52*$^{-/-}$ Av ratio	WT vs. *Fkbp52*$^{-/-}$ *P* (*t* test)	*Pgr*$^{-/-}$ vs. *Fkbp52*$^{-/-}$ Av ratio	*Pgr*$^{-/-}$ vs. *Fkbp52*$^{-/-}$ *P* (*t* test)	*P* (ANOVA)
Vimentin	P20152	53.5 5.1	1.00	0.93	1.28	0.017	1.28	0.005	0.008
Desmin	P31001	53.3 5.2	1.02	0.90	1.33	0.008	1.31	0.031	0.016
Aldehyde dehydrogenase, mitochondrial precursor	P47738	57.0 7.5	1.05	0.50	1.26	0.005	1.20	0.005	0.005
Eukaryotic initiation factor 4A-1	P29562	45.4 5.3	−1.03	0.79	1.19	0.028	1.22	0.003	0.016
Charged multivesicular body protein 2a	Q9DB34	25.1 5.9	−1.00	0.97	1.36	0.006	1.36	0.006	0.002
Indolethylamine N-methyltransferase	P40936	30.0 6.0	1.08	0.73	2.39	0.01	2.21	0.013	0.008